

Synthesis of Urea Calcium Phosphate via Ball Milling Technique

Nur Fairuzza Syahiera bt Fauzi, Atikah bt Kadri

Faculty of Chemical Engineering, Universiti Teknologi Mara,
40450 Shah Alam, Selangor, Malaysia.

Abstract— Urea calcium phosphate, $\text{CO}(\text{NH}_2)_2 \cdot \text{Ca}_3(\text{PO}_4)_2 \cdot \text{H}_2\text{O}$ was prepared using mixer ball mill by estimating the weight ratio of urea prills and calcium phosphate (monohydrate) powder. The structural properties and phase transformations of the synthesized substances were analysed by using Fourier Transform Infrared Spectroscopy (FTIR) and X-ray diffraction (XRD). Based on these analyses, this study suggested that urea calcium phosphate can be synthesized at 1:3 weight ratio of urea to calcium phosphate (monohydrate) at 10 minutes milling time.

Keywords— Urea, calcium phosphate, urea calcium phosphate, ball milling

I. INTRODUCTION

Urea, $\text{CH}_4\text{N}_2\text{O}$ and calcium phosphate, $[\text{Ca}_3(\text{PO}_4)_2]$ are used extensively in agriculture field as fertilizers as both compounds contain the main elements needed for plant growth and development, which are nitrogen (N) and phosphorus (P). Urea constitutes the highest amount of N compared to other N fertilizers whereas $[\text{Ca}_3(\text{PO}_4)_2]$ is known as a material that promotes slow release elements in the system. A research on the application of $[\text{Ca}_3(\text{PO}_4)_2]$ coatings in drug delivery system proves that $[\text{Ca}_3(\text{PO}_4)_2]$ promotes longer availability of the implant materials.^[1]

However, nitrification of ammonium (NH_4^+), hydrolysis of urea and ammonia (NH_3) volatilization^[2] as well as reversion of phosphate (PO_4^{3-}) back to rock phosphate occur naturally over time. Therefore, in order to overcome this problem, synthesizing a new type of enhanced efficiency fertilizer (EEF) by introducing phosphate additive material to urea can reduce nutrient losses to the environment. Besides, EEF also able to provide longer nutrients availability as EEF can delay the release of nutrients for plant uptake.

The objective of this research is to synthesis urea calcium phosphate via ball milling technique, by estimating the weight ratio of urea to calcium phosphate. These crystalline and odorless powders can be synthesized by the proposed technique as ball milling is a process that uses mechanical energy from the grinding balls to activate chemical reactions and structural changes of the materials.^[3] The reaction equation used to synthesis urea calcium phosphate can be written as



Besides being able to deform, fracture and cold welding particles to produce products that are in fine powder forms, ball milling also provides direct reaction routes, therefore this technique is design to reduce energy consumptions. Moreover, this technique also allows the synthesis reaction to be done at room temperature without transitioning phases and the need to use solvents.^[4]

FTIR spectroscopy displays the peak absorbance values in an infrared spectrum and the values obtained are used to identify the presence of functional groups in a compound. Figure 1 below shows the ranges of wavenumbers based on the molecular structures of a substance.

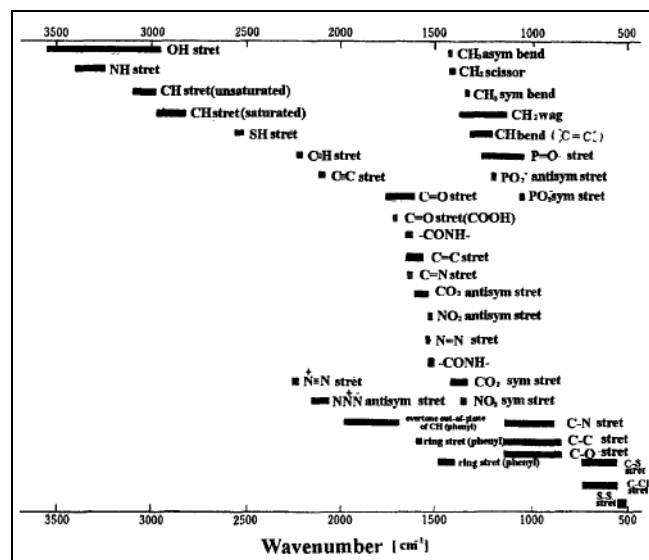


Figure 1: Frequency of functional groups based on the wavenumber.^[5]

On the other hand, XRD is a technique used to identify the phase, orientation and the lattice parameter, as well as the quality and the structure of the crystal. This method of analysis uses monochromatic x-ray beam generated by a cathode ray tube filter to interfere with the crystalline samples. As a result of this powder diffraction pattern, the characteristics of the analysed substance can be defined by observing the peak positions and intensities.^[6] This is because the diffraction patterns generate a unique fingerprint of the crystals present in the sample.

II. METHODOLOGY

A. Study Design

In this experiment, the raw materials used are urea prills (manufactured by Petronas) and chemically pure calcium phosphate (monohydrate) $[\text{Ca}(\text{H}_2\text{PO}_4)_2 \cdot \text{H}_2\text{O}]$ (manufactured by R&M Chemicals). These compounds were measured using Shimadzu weighing machine (Model: AY220) and mixed at 4 different weight ratios (Table 1). The mill was filled with 32.162 g of stainless steel grinding balls to powder at the ratio of 20:1.

Table 1: Weight ratio of $\text{CH}_4\text{N}_2\text{O}$ to $\text{Ca}(\text{H}_2\text{PO}_4)_2 \cdot \text{H}_2\text{O}$.

Sample	Ratio	
	$\text{CH}_4\text{N}_2\text{O}$	$\text{Ca}(\text{H}_2\text{PO}_4)_2 \cdot \text{H}_2\text{O}$
A	1	1
B	1	2
C	1	3
D	1	4

The synthesis of this nanomaterial was carried out by using Retsch laboratory scale mixer ball mill (Model: MM400) at 4 different milling times, t which are 4, 8, 10 and 15 min, whereas the frequency, f of the ball mill was kept constant at 30 Hz throughout the experiment. The unknown samples obtained were then analysed by using FTIR spectroscopy and XRD.

FTIR spectroscopy able to detect the changes in the structure and bonding of urea, pure calcium phosphate (monohydrate) as well as the unknown samples acquired from the milling process. For FTIR analysis, each sample were analysed on Shimadzu FTIR Spectroscopy at room temperature with the frequency range of $4000 - 515 \text{ cm}^{-1}$.

The samples were then analysed by using PANanalytical XRD (Model: ExpertPRO). The instrument was operated in a continuous mode and scanned over a 2θ range of 10° to 90° . The samples were irradiated with monochromatic $\text{Cu K}\alpha$ radiation of $\lambda = 1.542 \text{ \AA}$. Each analysis requires about 1 g sample.

III. RESULTS AND DISCUSSION

A. FTIR Analysis

Infrared (IR) spectroscopy is based on the vibrations of the atoms in a molecule. When a molecule absorbs infrared radiation, the chemical bonds vibrate to stretch or bend [7]. Stretching vibration indicates the change in bond length while bending vibration indicates the change in the bond angle. The graphs were plotted based on the relationship between wavenumber against %Transmittance.

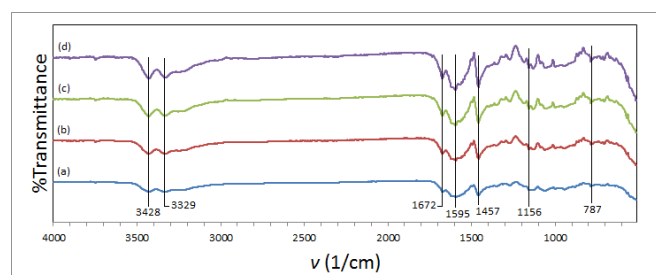


Figure 2: FTIR spectra of $\text{CH}_4\text{N}_2\text{O}$ milled at (a) $t = 4$ min (b) $t = 8$ min (c) $t = 10$ min (d) $t = 15$ min.

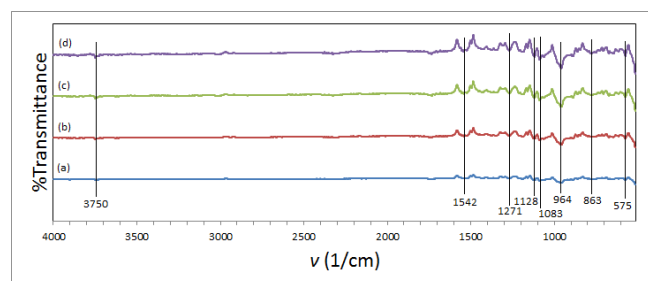


Figure 3: FTIR spectra of $\text{Ca}(\text{H}_2\text{PO}_4)_2 \cdot \text{H}_2\text{O}$ milled at (a) $t = 4$ min (b) $t = 8$ min (c) $t = 10$ min (d) $t = 15$ min.

Figure 2 and Figure 3 illustrates the absorbance peaks of $\text{CH}_4\text{N}_2\text{O}$ and $\text{Ca}(\text{H}_2\text{PO}_4)_2 \cdot \text{H}_2\text{O}$. The FTIR peaks are similar though the substances were milled at different times. Therefore, it is safe to presume that the structural changes of both materials are independent on the milling time.

FTIR spectra of $\text{CH}_4\text{N}_2\text{O}$ and $\text{Ca}(\text{H}_2\text{PO}_4)_2 \cdot \text{H}_2\text{O}$ samples were summarized in Table 1 and Table 2, respectively. These absorbance values were compared to analysis done in previous works [7-10]. Apart from these peaks, small absorption bands from $4000 - 3000 \text{ cm}^{-1}$ appeared due to presence of O-H bond in water.

Table 1: Infrared absorption bands, ν for $\text{CH}_4\text{N}_2\text{O}$.

Experimental data	$\nu \text{ (cm}^{-1}\text{)}$		Assignment
	M. K. Trivedi <i>et al.</i> (2015) [7]	Z. Piasek <i>et al.</i> (1962) [8]	
3428, 3329	3428	3456, 3350	N-H stretch
-	2359	-	CO_2 absorption
1672	1684	1687	C=O stretch
1595	1624	1627	C-N-H bend
1457	1458, 1003	1465	C-N asym stretch
1156	1155	1155, 1055	NH_2 bend
787	787	790	NH_2 bend (out of plane)

Table 2: Infrared absorption bands, ν for $\text{Ca}(\text{H}_2\text{PO}_4)_2 \cdot \text{H}_2\text{O}$.

Experimental data	$\nu \text{ (cm}^{-1}\text{)}$		Assignment
	J. Sánchez-Enríquez <i>et al.</i> (2013) [9]	B. Boonchom <i>et al.</i> (2009) [10]	
3750	3461 – 3220	3242, 3464	O-H stretch
-	2934	2926	(P)O-H stretch
1271	1240	1240	P-O-H bend
1128	1128	1111	PO_2 asym stretch
1083	1066	1052	PO_2 sym stretch
964	975 – 962	960	$\text{P}(\text{OH})_2$ asym stretch
863	870	863	$\text{P}(\text{OH})_2$ sym stretch
575	576 – 524	540	PO_2 bend

Note: sym = symmetrical; asym = asymmetrical

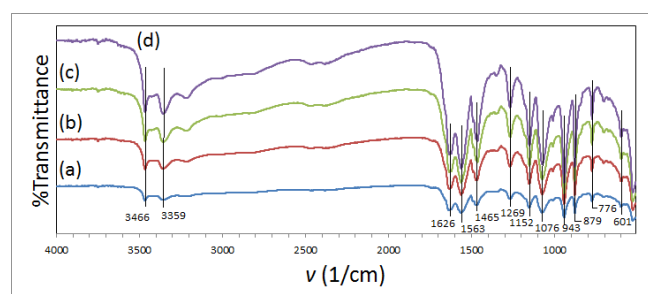


Figure 4: FTIR spectra of sample A milled at (a) $t = 4$ min (b) $t = 8$ min (c) $t = 10$ min (d) $t = 15$ min.

For sample A, similar absorption bands can be seen in Figure 4 though the substances were milled at different times. The stretching vibrations of O-H bonds are observed at 3466 cm^{-1} while the stretching vibrations of N-H bonds are observed at 3359 cm^{-1} . Another peak at 1626 cm^{-1} and 1563 cm^{-1} appeared at higher intensity in the spectra. This band represents stretching vibrations of C=O and bending vibrations of C-N-H bond, respectively. On the other hand, C-N stretching vibrations displayed at 1465 cm^{-1} , NH₂ bending vibrations at 1152 cm^{-1} and PO₂ symmetrical stretching vibrations at 1076 cm^{-1} . P(OH)₂ asymmetrical and symmetrical stretching vibrations can be seen at bands 943 cm^{-1} and 879 cm^{-1} , respectively. At 776 cm^{-1} , there a deformation of NH₂ bending out of the plane while 601 cm^{-1} signifies the bending of C-H bond in the compound [11].

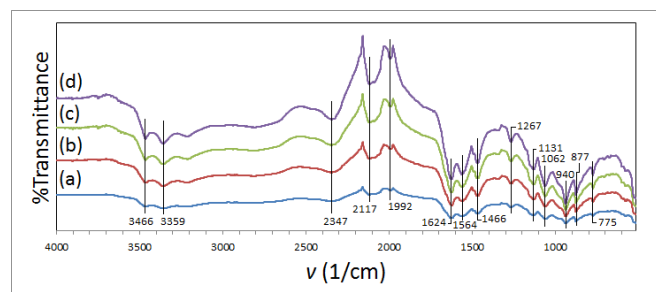


Figure 5: FTIR spectra of sample B milled at (a) $t = 4$ min (b) $t = 8$ min (c) $t = 10$ min (d) $t = 15$ min.

From Figure 5, sample B shows the stretching of O-H bonds at 3466 cm^{-1} and stretching of N-H bonds at 3359 cm^{-1} . Other peaks showed CO₂ absorption stretch at 2347 cm^{-1} , formation of bond -N=C=O at 2117 cm^{-1} , C=C asymmetrical stretching vibrations of alkenes at 1992 cm^{-1} , C=O stretching vibrations at 1624 cm^{-1} , C-N-H bending at 1564 cm^{-1} , C-N stretching vibrations at 1466 cm^{-1} , NH₂ bending vibrations at 1131 cm^{-1} and NH₂ bending out of plane vibrations at 775 cm^{-1} were detected in sample B. Based on Table 1 and 2, 1062 cm^{-1} represents PO₂ symmetrical stretching. Also, 940 cm^{-1} and 877 cm^{-1} signifies the presence of P(OH)₂ asymmetrical and symmetrical stretching vibrations respectively.

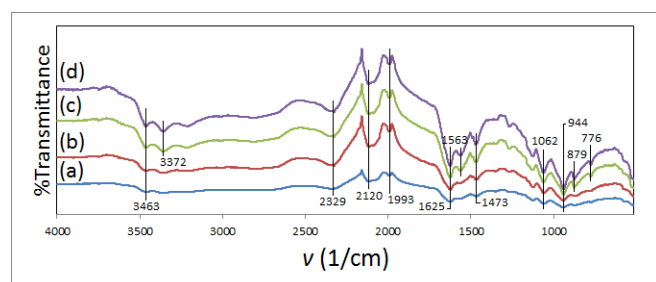


Figure 6: FTIR spectra of sample C milled at (a) $t = 4$ min (b) $t = 8$ min (c) $t = 10$ min (d) $t = 15$ min.

FTIR pattern of sample C for different milling times by mixer ball mill are shown in Figure 6. O-H and N-H stretching vibrations bands appeared at $\nu = 3463\text{ cm}^{-1}$ and 3372 cm^{-1} , respectively. Other peaks show $\nu = 2120\text{ cm}^{-1}$ for stretching of -N=C=O , $\nu = 1993\text{ cm}^{-1}$ for C=C stretching of alkenes, $\nu = 1625\text{ cm}^{-1}$ for C=O stretching, 1563 cm^{-1} for C-N-H bending, $\nu = 1473\text{ cm}^{-1}$ for C-N stretching of alkanes, $\nu = 1125\text{ cm}^{-1}$ for NH₂ bending, $\nu = 1062\text{ cm}^{-1}$ for PO₂ asymmetrical stretching, $\nu = 944\text{ cm}^{-1}$ and 879 cm^{-1} for P(OH)₂ asymmetrical and symmetrical stretching and $\nu = 776\text{ cm}^{-1}$ for NH₂ bending out of the plane. CO₂ absorption bands can be seen at $\nu = 2329\text{ cm}^{-1}$.

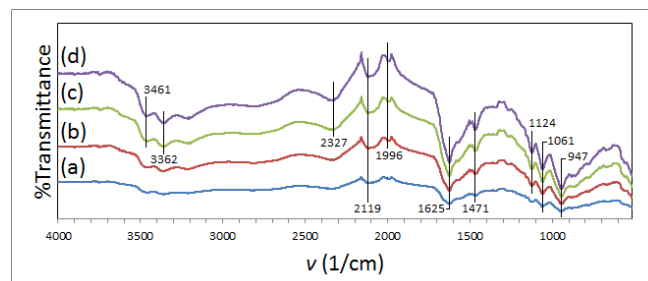


Figure 7: FTIR spectra of sample D milled at (a) $t = 4$ min (b) $t = 8$ min (c) $t = 10$ min (d) $t = 15$ min.

Absorption peaks in Figure 7 showed O-H stretching at 3461 cm^{-1} ; N-H stretching at 3362 cm^{-1} ; CO₂ absorption bands at 2327 cm^{-1} ; -N=C=O stretching at 2119 cm^{-1} ; C=C stretching of alkenes at 1996 cm^{-1} ; C=O stretching at 1625 cm^{-1} ; C-N stretching of alkanes at 1471 cm^{-1} ; NH₂ bending at 1124 cm^{-1} ; PO₂ symmetrical stretching at 1061 cm^{-1} and P(OH)₂ asymmetrical stretching at 947 cm^{-1} . As referred to Table 1 and 2, the experimental data were tabulated in Table 3 below.

Table 3: Infrared absorption bands, ν for sample A, B, C and D after milling process.

Assignment	$\nu\text{ (cm}^{-1}\text{)}$			
	A	B	C	D
O-H stretch	3466	3466	3463	3461
N-H stretch	3359	3359	3372	3362
CO ₂ absorption	-	2347	2329	2327
-N=C=O stretch	-	2117	2120	2119
C=C stretch	-	1992	1993	1996
C=O stretch	1626	1624	1625	1625
C-N-H bend	1563	1564	1563	-
C-N stretch	1465	1466	1473	1471
NH ₂ bend	1152	1131	1125	1124
PO ₂ sym stretch	1076	1062	1062	1061
P(OH) ₂ asym stretch	943	940	944	947
P(OH) ₂ sym stretch	879	877	879	-
NH ₂ bend	776	775	776	-
C-H bend	601	-	-	-

Based on Table 3, it can be presumed that the O-H stretching frequency appeared in the spectra may be due to the presence of water molecule in $\text{Ca}(\text{H}_2\text{PO}_4)_2 \cdot \text{H}_2\text{O}$ compound. The N-H stretching frequency increases from 3429 cm^{-1} as delocalization of electrons may occur during the process, resulting in higher wavelength. The formation of new bonds occurs in a molecule during elimination process by atom removal. This reaction happened during the synthesis process in sample B, C and D as there are development of -N=C=O and C=C bonds.

Apart from that, the frequency of C=O bond, PO₂ symmetrical and P(OH)₂ asymmetrical stretching vibration values decrease. These occurrences may be due to the change in the bond length after the milling process. Data also showed that the C-N-H and NH₂ bending vibration decreases that might be due to the alteration of the bond angle in the groups. Comparing the samples to the precursor, it can also be seen that the stretching of C-N and P(OH)₂ symmetrical increases from 1457 cm^{-1} and 863 cm^{-1} , respectively. The changes of the wavelengths may cause by the modification of the bond length in the functional group. (reason why change/what happened during the process).

B. XRD Analysis

For XRD analysis, the graph was plotted between the relationships of angle of diffraction, 2θ against the intensity.

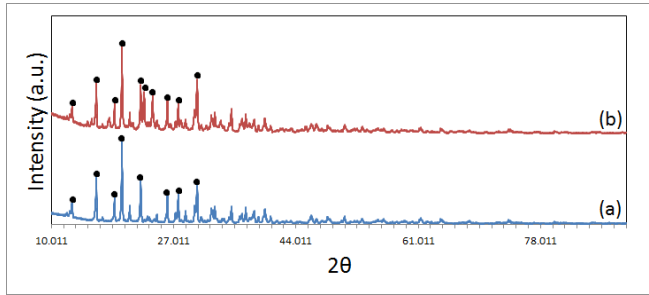


Figure 6: XRD pattern of (a) $\text{CH}_4\text{N}_2\text{O}$ (b) $\text{Ca}(\text{H}_2\text{PO}_4)_2 \cdot \text{H}_2\text{O}$ milled at $t = 10$ min.

For $\text{CH}_4\text{N}_2\text{O}$, XRD pattern (curve (a) Fig. 6) shows peaks at 2θ diffraction angles of 12.88° , 16.27° , 18.80° , 19.82° , 22.40° , 26.13° , 27.66° and 30.26° . Meanwhile, XRD pattern for $\text{Ca}(\text{H}_2\text{PO}_4)_2 \cdot \text{H}_2\text{O}$ (curve (b) Fig. 6) shows peaks at 2θ diffraction angles of 12.87° , 16.23° , 18.82° , 19.80° , 22.46° , 22.90° , 24.09° , 26.13° , 27.64° and 30.24° .

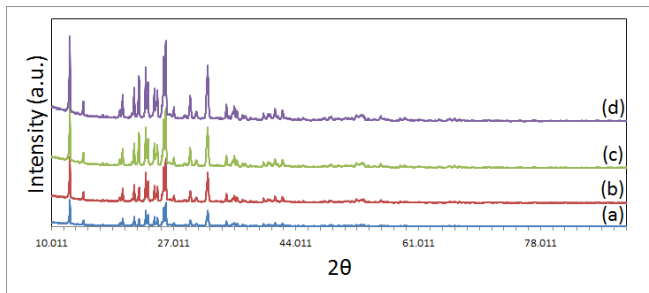


Figure 7: XRD pattern of sample A milled at (a) $t = 4$ min (b) $t = 8$ min (c) $t = 10$ min (d) $t = 15$ min.

All curves in Figure 7 show significant peaks at $2\theta = 12.6^\circ$, 14.5° , 19.9° , 21.5° , 22.2° , 23.2° , 24.3° , 25.6° , 25.9° and 31.7° . These angles are almost as similar to the precursor (Figure 6), which signifies no formation of new bonds during the synthesis.

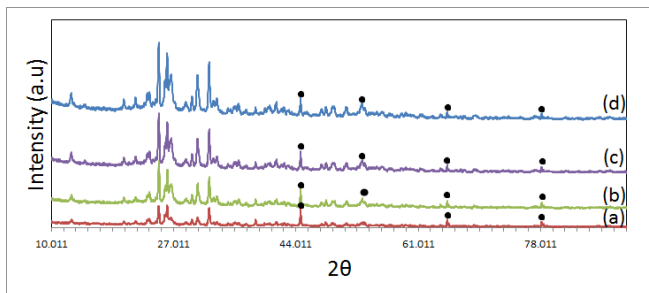


Figure 8: XRD pattern of sample B milled at (a) $t = 4$ min (b) $t = 8$ min (c) $t = 10$ min (d) $t = 15$ min.

All curves on Figure 8 show significant peaks at $2\theta = 12.8^\circ$, 24.9° , 26.1° , 26.7° , 30.3° and 31.9° . However, as compared to Figure 6, there are new peaks formed at $2\theta = 44.6^\circ$, 53.2° , 65.0° and 78.2° . This indicates that $\text{CO}(\text{NH}_2)_2 \cdot \text{Ca}_3(\text{PO}_4)_2 \cdot \text{H}_2\text{O}$ peaks start to develop when $\text{Ca}(\text{H}_2\text{PO}_4)_2 \cdot \text{H}_2\text{O}$ is added to $\text{CH}_4\text{N}_2\text{O}$ at the weight ratio of 2:1.

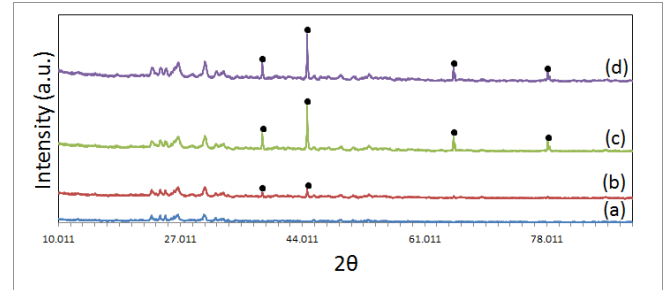


Figure 9: XRD pattern of sample C milled at (a) $t = 4$ min (b) $t = 8$ min (c) $t = 10$ min (d) $t = 15$ min.

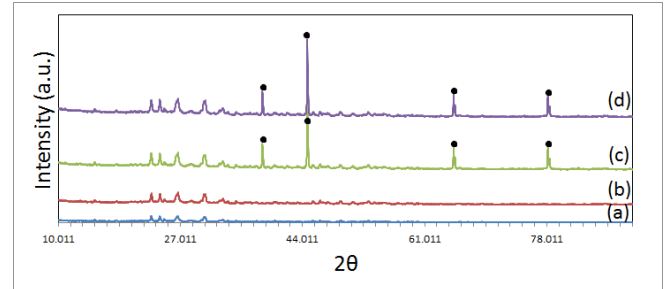


Figure 10: XRD pattern of sample D milled at (a) $t = 4$ min (b) $t = 8$ min (c) $t = 10$ min (d) $t = 15$ min.

Figure 9 and 10 above show the diffraction peaks of sample C and D at milling time, $t = 4, 8, 10$ and 15 minutes. As compared to Figure 6, new peaks are observed (curve (c) and (d) Fig. 9 and 10) at $2\theta = 38.4^\circ$, 44.7° , 65.1° and 78.2° . This denotes the appearance of new bonds between $\text{CH}_4\text{N}_2\text{O}$ and $\text{Ca}(\text{H}_2\text{PO}_4)_2 \cdot \text{H}_2\text{O}$ structure. The intensity of the peaks increased over milling time as the crystallinity of the substance increases.

The synthesis of urea calcium phosphate can be described as decomposition, deformation and refining of urea and calcium phosphate by mechanical energy from the grinding balls. Based on FTIR and XRD analyses, there is possibility of these two raw materials to combine to produce urea calcium phosphate. By comparing all the collected data, it is suggested that milling $\text{CH}_4\text{N}_2\text{O}$ and $\text{Ca}(\text{H}_2\text{PO}_4)_2 \cdot \text{H}_2\text{O}$ at weight ratio of 1:3 at $t = 10$ minutes can create $\text{Ca}_3(\text{PO}_4)_2 \cdot \text{CO}(\text{NH}_2)_2 \cdot \text{H}_2\text{O}$. This is because the substance synthesized exhibits new and high diffraction peaks as shown in Figure 9 (c). In addition, based on Table 3, FTIR analysis also proves that there are formations of new bonds at that particular time and ratio.

IV. CONCLUSION

The results of this work provide a particular set of data that specify the characteristic of diffraction peaks and phases of urea calcium phosphate

In this work, urea calcium phosphate were successfully synthesized by ball milling 1:3 weight ratio of urea to calcium phosphate (monohydrate) at $t = 10$ minutes and $f = 30$ Hz. The experimental method is simple and fast as this technique can be carried out consistently at room temperature. Detailed analyses have been carried out by FTIR spectroscopy and XRD techniques.

FTIR analyses propose that the structural changes of these substances are independent to the milling time, but highly dependent on the weight ratio of the raw materials used. Meanwhile, XRD analyses complement the results obtained from FTIR spectra.

ACKNOWLEDGMENT

The author would like to gratefully thank Atikah bt Kadri as the supervisor for this work. Also, a huge gratitude expressed to Universiti Teknologi Mara for providing the instrumental facilities in order to complete this work.

References

- [1] Zhang, X., & Cresswell, M. (2016). Calcium Phosphate Materials for Controlled Release Systems. *Inorganic Controlled Release Technology*, 161-187. doi:10.1016/b978-0-08-099991-3.00006-5
- [2] Cajuste, L. J., Sánchez-A, E., & Laird, R. J. (1996). Behaviour of urea and ammonium sulfate fertilizers and their N uptake relationships in calcareous soils. *Nitrogen Economy in Tropical Soils*, 347-353. doi:10.1007/978-94-009-1706-4_33
- [3] McCormick, P. G., & Froes, F. H. (1998). The fundamentals of mechanochemical processing. *Jom*, 50(11), 61-65. doi:10.1007/s11837-998-0290-x
- [4] Sopicka-Lizer, M. (2010). Introduction to mechanochemical processing. *High-energy ball milling mechanochemical processing of nanopowders*. Cambridge: Woodhead Publishing Limited.
- [5] Christy, A. A., Ozaki, Y., & Gregoriou, V. G. (2001). *Modern Fourier transform infrared spectroscopy*. Amsterdam: Elsevier.
- [6] Lee, M. (2016). *X-ray diffraction for materials research from fundamentals to applications*. Oakville, ON: Apple Academic Press.
- [7] Trivedi, M. K. (2015). An Impact of Biofield Treatment on Spectroscopic Characterization of Pharmaceutical Compounds. *Modern Chemistry & Applications*, 03(03). doi:10.4172/2329-6798.1000159
- [8] Piasek, Z., & Urbanski, T. (1962). The Infra-red Absorption Spectrum and Structure of Urea. *BULLETIN EE L'ACADEMIE POLONAISE DES SCIENCES*, X(3).
- [9] Sánchez-Enríquez, J., & Reyes-Gasga, J. (2013). Obtaining Ca(H₂PO₄)₂·H₂O, monocalcium phosphate monohydrate, via monetite from brushite by using sonication. *Ultrasonics Sonochemistry*, 20(3), 948-954. doi:10.1016/j.ultsonch.2012.10.019
- [10] Boonchom, B., & Danvirutai, C. (2009). The morphology and thermal behavior of Calcium dihydrogen phosphate monohydrate (Ca(H₂PO₄)₂·H₂O) obtained by a rapid precipitation route at ambient temperature in different media. *Journal of Optoelectronics and Biomedical Materials*, 1(1), 115-123.
- [11] Kennepohl, D., Farmer, S., & Reusch, W. (2019, May 23). 13.4: Infrared Spectra of Some Common Functional Groups. Retrieved from [https://chem.libretexts.org/Bookshelves/Organic_Chemistry/Map:_Organic_Chemistry_\(Wade\)/13:_Infrared_Spectroscopy_and_Mass_Spectrometry/12.08:_Characteristic_Absorptions_of_Alcohols_and_Amines](https://chem.libretexts.org/Bookshelves/Organic_Chemistry/Map:_Organic_Chemistry_(Wade)/13:_Infrared_Spectroscopy_and_Mass_Spectrometry/12.08:_Characteristic_Absorptions_of_Alcohols_and_Amines)
- [12] Glagovich, N. (2005, January 03). Infrared Spectroscopy. Retrieved from http://www.instruction.greenriver.edu/kmarr/chem162/Chem162_Labs/Interpreting_IR_Spectra/IR_Absorptions_for_Functional_Groups.htm